Association Journal of Interdisciplinary Technics in Engineering Mechanics, Vol. 2, No. 3, 2024
ISSN: 3049-0898

Fluid Mechanics for Mechanical Engineers: Fundamentals and Applications

Dr. Amit Verma[1] and Dr. Renu Chandra[2]*

[1]Department of Mechanical Engineering, Shree Ram Institute of Engineering and Technology, Lucknow, India.*

[2]Department of Mechanical Engineering, Shree Ram Institute of Engineering and Technology, Lucknow, India.

Abstract--- Understanding the capabilities and changes of platelets and whole blood, as well as the interactions between platelets and the arterial wall, is crucial in the cardiovascular system, where biofluid mechanics plays a major role. Important aspects of central liquid mechanics that are important for comprehending the bloodstream in the context of the human circulatory system are presented. Experiments have shown how hemodynamics can affect the healing of varicose veins and aneurysms. A few other elements, including the vessel wall's construction, are also important. Basic analyses have demonstrated that the stream conduct is determined by the vessel wall's flexibility and calculation. Significant variations in speed indicate stream irritations that should be avoided. Physicians should understand hydrodynamic parameters such as shear loads, speed slopes, tensions, and stream proportions. They need also understand how the stream behaves in comparison to the wall and platelets, as well as speed disseminations. Platelets and lipids are the main cause of atherosclerosis, and these mechanical components are essentially responsible for their testimony. Plaques and aggregates are the result of blood cells interacting with blood arteries. These deposits are mostly located in artery bends and branches where there are areas of flow separation, secondary flows, and interruptions in blood flow. We provide studies on hemodynamic effects using flow wires, stents, or vascular surgical patches in an elastic silicone rubber model of the cardiovascular system. These investigations could be crucial for enhancing therapeutic and diagnostic uses.

Keywords--- Fluid Mechanical, Biofluid Mechanics.

Received: 10 - 06 - 2024; Revised: 05 - 07 - 2024; Accepted: 16 - 08 - 2024; Published: 30 - 09 - 2024

I. Introduction

The kinematics and components of human, animal, and plant bodily fluids are illustrated in liquid mechanics. It detects both internal bodily movements, like blood flowing through veins, and external ones, like a bird's flight or the movement of air around the body in a cooling system (Turkyilmazoglu, 2020). Hemodynamics controls bodily fluids. The estimation of tension, stream, and obstruction is handled by traditional hemodynamics both in vivo and ex vivo. Nearby time-subordinate speeds and streams in veins, the respiratory system, the lymphatic system, and the microcirculation are measured and broken down by current biofluid mechanics. Significant progress has recently been made in the fields of liquid mechanics, acoustics, and computational and experimental research in the realm of biomedical design. High-end equipment, sophisticated computational techniques, and innovative imaging techniques have made these advancements possible (Feng et al., 2020). The development of modern design processes and numerical devices is influenced by computational tools. The discoveries have aggressively spurred new treatments aimed at improving human wellbeing and contribute to a deeper understanding of physiological cycles in the circulatory and respiratory systems as well as voice development. These advancements include, but are not limited to, early infection detection, monitoring of disease transmission, personalized treatments, meticulous planning, effective drug delivery, and novel medical devices. The development of both trial and computational methods depends on the collaborative energy of computational tools and exploratory diagnostics. To approve computational liquid elements (CFD) and modify each stage of the CFD interaction to achieve reliable results, precise exploratory data is essential (Cai et al., 2021). By contributing vast amounts of data, CFD aids in trial arrangement planning and contributes to a deeper understanding of exploratory results.

II. Related Work

Cai et al., (2021) attempted an AI (ML) computation that depicts a cycle to section patient-explicit four-layered stage contrast attractive reverberation imaging (4D-PCMRI) of the thoracic aorta, taking into consideration the clinical significance of FSI evaluation of aortic blood stream in patients with bicuspid aortic valve (BAV). Six people were used by the experts; three of them had a nonstenotic usable bicuspid aortic valve (BAV), and three of them had a nonstenotic tricuspid aortic valve (TAV). They considered the stream field characteristics of the two groups using a division based on Total Segmentator. In comparison to BAV, they displayed more grounded vortex activity in the proximal ascending aorta of TAV patients, which resulted in higher distracting shear pressure. Garnier et al., (2021) portrayed the utilization of blood spot imaging (BSI) in view of echocardiographic information to analyze preoperative and postoperative stream designs after subaortic resection and aortic valve fix. Information showed that stream reflux was diminished after a medical procedure, bringing about changes in wall shear pressure. The time-arrived at the midpoint of wall shear pressure (TAWSS) didn't change, yet the oscillatory shear record (OSI) diminished, recommending a lower hazard of harm to the aortic wall and valve leaflets (Liu et al., 2021). They fostered a carotid bifurcation model with a "solid" and a "inclined" calculation and utilized CFD to look at the two coming about stream fields. They showed that in the "sound" math, clip vortex structures foster in the inside carotid sinus (ICA) and endure for a huge piece of the cardiovascular cycle.

Include the stomach, renal, femoral, coronary, and carotid conduits in the various silicone elastic models of the aortic curve. From these detailed macroscopic measurements, the shear stress can be calculated very accurately. Shear stress acts on the endothelium as well as the medial membrane. Particles and blood cells in the recirculation zones require closer inspection (Brunton, 2021). They usually do not remain long in the flow separation zones, but some particles or particle aggregates may rotate for several periods within these zones, as visualized by stress optics using birefringent solutions. This design appears early in the cycle as a "inclined" mathematical construction and persists for a much shorter time, followed by less well-coordinated structures. Stream examples and the testimony of tiny/nano particles in real-world human nasal sections during septoplasty are affected by septal deviation (Alexandersen & Andreasen, 2020). The authors used Eulerian and Lagrangian methodologies for nano- and microparticles to simulate a consistent wind current through the nasal passages. The stream field and molecular statement are displayed as part of the entrance calculation in the reenactment results (Brunton et al, 2020). For microparticles, the deposition rate in a deviated septum is higher than in normal and postoperative passages. At the same time, nanoparticle deposition shows similar trends during both normal and postoperative time courses, making the simulation a suitable tool to predict intranasal airflow and particle deposition patterns that will occur during a given surgical procedure (Elger et al., 2022).

III. Methodology

A blood simple with a refractive record equal to the model walls was cultivated in order to replicate the stream characteristics of blood. Watery dimethyl sulfoxide doped with various polyacrylamides (0.0035% Separan AP-302 and 0.0025% AP-45, Dow Substance) made up 51 weight percent of the liquid. This liquid behaves rheologically similarly to blood at 46% hematocrit. At 21°C, Figure 2 (top) plots the model liquids' thickness vs shear rate.

Applications of Biomedicine and Liquid Mechanics

Computational fluid dynamics is often used to solve complex problems in the biomedical field. CFD is becoming a key element in developing modern designs and optimizations through computer-aided simulations, leading to reduced operational costs and increased efficiency. Many simulations and clinical results have been used to investigate analysis in biomedical applications, especially related to blood flow and nasal airflow. Blood flow analysis studies include ventricular function, coronary arteries, and blood circulation in heart valves. Nasal airflow analysis includes basic airflow in the human nasal cavity, improved drug delivery, and virtual surgery.

Table 1: Material of Brake Components

Part Name	Material
Casing & Casing cap	SAE 1020 steel
Rotor	SAE 1020 steel
Bobbin	316 Stainless steel (Non-magnetic)
Rotor shaft	SS 304 Stainless steel (Non-magnetic) MR Fluid Commercial

To provide slowing down obstruction, the electromagnet's generated attractive field should pass through the MRF in the hole between the rotor and the lodging. In order to ensure that the attractive motion thickness is grouped inside the MRF, the lodging, lodging cover, and rotor—which structure the attractive field—need to have strong penetrability. Because SAE 1020 steel is readily available, reasonably priced, and has many desirable qualities, it was selected as the material for these parts. The rotor shaft is composed of an unappealing material to prevent the spilling of enticing motion. The curls are also made of unappealing material because they don't participate in the slowing down force or attractive transition mindset. The different materials used for the MR brake are listed in Table 1.

Utilizing Commercial MR Liquid, MR Brake

Field-actuated slowing down and demagnetizing slowing down force, force proportion, hysteresis duration, force following control characteristics, speed hang, and other factors are used to estimate the display of MR brakes. This study examined the force proportion, speed hang, and field-actuated and demagnetizing slowing down force of MR brakes.

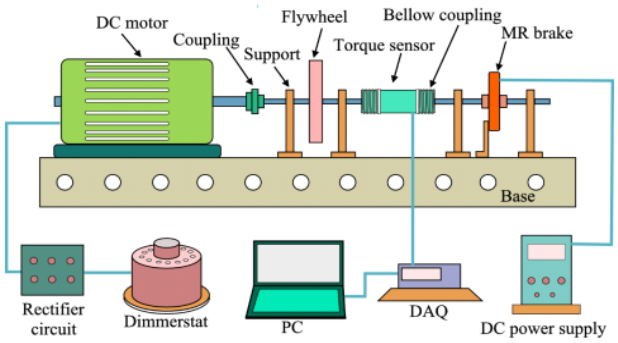

Figure 1: Diagrammatic Representation of the MR Braking Test Configuration

Figure 1 shows the schematic graph for the MR braking test setup. It consists of a DC engine connected to the MR brake in turn by means of a flywheel, a Howls grip, a Lovejoy grasp, and a force sensor. A DC engine was used for speed control since it is easier and more accurate to manage than an air conditioner engine.

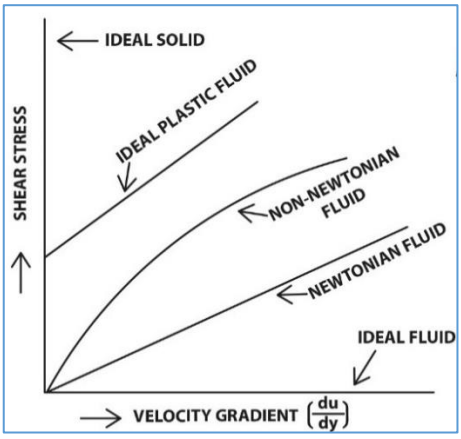

Figure 2: Types of Fluid

The DC engine is associated with a rectifier circuit, which gets power from a dimmer stat. The dimmer stat is controlled from the 220 V organization. The dimmer stat is utilized to fluctuate the speed of the engine by controlling the current provided to the DC engine. The result of the dimmer is associated with a rectifier circuit that switches AC over completely to DC to drive a DC engine.

IV. Result and Discussions

The mass portion of iron particles in the liquid overall influences the normal recurrence and damping coefficient of the bars, according to the vibration characteristics of MR radiates loaded with two types of commercially available MRFs. The vibration conduct of MRF sandwich radiates using natively manufactured MRFs with different mass divisions and molecule sizes of iron particles has not been extensively studied in that mindset. The effects of molecule size and mass portion on the damping proportion and normal recurrence characteristics of MR liquid cored sandwich radiates were investigated in this review. Additionally, it was suggested that sandwich structures with MR liquid centers have the best MR liquid structure.

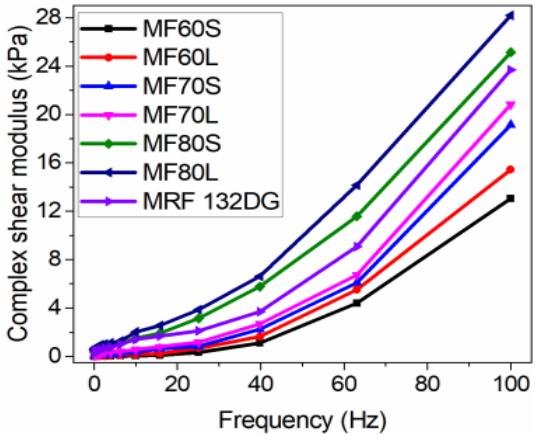

Figure 3: Commercial and in-House MRFs at 0 Gauss

The complex shear modulus with recurrence varies for different MRFs at 0 and 745 Gauss, separately, as shown in Figure 3. The capacity modulus, misery modulus, and complex shear modulus tend to increase with recurrence in the off state (0A). In the off state, the misfortune modulus is practically greater than the capacity modulus, suggesting that the MRF behaves viscously rather than flexibly. The opposite behavior is observed in the on express when the MRF transitions into a semi-strong state. As a result, the capacity modulus increases further in comparison to the misfortune modulus.

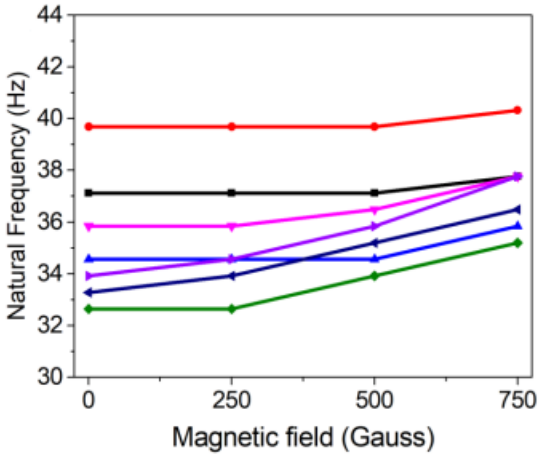

Figure 4: First Natural Frequency Variation with Magnetic Field

The development of the first three regular frequencies and damping proportions of the bar loaded with the commercial MR liquid MRF 132DG and the pre-arranged MRF are depicted in Figure 4. The damping proportion

increases as the applied attractive field grows. Additionally, when the attractive field expands, the normal frequencies move upward and are higher than the major normal recurrence for the second and third regular frequencies. This is due to the bar's subsequent solidity and the expansion away modulus with an expanding attractive field. Particularly for the higher modes, the regular frequencies of the MRF with the higher mass portion of CIP are lower. This is based on the idea that a decrease in recurrence results from the bar mass increasing with the expanding mass component. Additionally, the damping proportion increases overall as the mass fraction of CIP grows, and more grounded MR impact occurs due to the presence of more iron particles. In all attractive fields, the LCIP-MRF pillar's damping proportion is greater than the SCIP shaft's due to its larger complex shear modulus and higher immersion charge.

V. Conclusion

Three mass parts of iron powder and two iron molecule sizes were used to arrange six MRFs. Vibration experiments using a rheometer were used to determine the viscoelastic characteristics of the pre-arranged MRFs and business MR liquid MRF 132DG (Ruler Partnership). Six of the developed MRFs and business MR liquid MRF 132DG (Master Organization) were put onto seven MRF sandwich radiates. To determine the normal frequencies and damping proportions of the cantilevered MRF sandwich radiates, influence hammer trials were conducted at different attractive fields. In addition, the ability to conceal vibrations was investigated by estimating the response of the MRF sandwich radiates under sinusoidal excitation. A flexible silicone elastic model of the circulatory system with flowwires, stents, or patches for vascular medical procedures is used to investigate the hemodynamic effects. These studies could be important for developing useful and analytical applications.

References

[1] Turkyilmazoglu, M. (2020). Single phase nanofluids in fluid mechanics and their hydrodynamic linear stability analysis. *Computer Methods and Programs in Biomedicine*, *187*, 105171. https://doi.org/10.1016/j.cmpb.2019.105171

[2] Feng, Y. J., Gao, Y. T., Li, L. Q., & Jia, T. T. (2020). Bilinear form, solitons, breathers and lumps of a (3+ 1)-dimensional generalized Konopelchenko–Dubrovsky–Kaup–Kupershmidt equation in ocean dynamics, fluid mechanics and plasma physics. *The European Physical Journal Plus*, *135*(3), 1-12. https://doi.org/10.1140/epjp/s13360-020-00204-2

[3] Cai, S., Mao, Z., Wang, Z., Yin, M., & Karniadakis, G. E. (2021). Physics-informed neural networks (PINNs) for fluid mechanics: A review. *Acta Mechanica Sinica*, *37*(12), 1727-1738. https://doi.org/10.1007/s10409-021-01148-1

[4] Cai, S., Wang, Z., Fuest, F., Jeon, Y. J., Gray, C., & Karniadakis, G. E. (2021). Flow over an espresso cup: inferring 3-D velocity and pressure fields from tomographic background oriented Schlieren via physics-informed neural networks. *Journal of Fluid Mechanics*, *915*, A102. https://doi.org/10.1017/jfm.2021.135

[5] Garnier, P., Viquerat, J., Rabault, J., Larcher, A., Kuhnle, A., & Hachem, E. (2021). A review on deep reinforcement learning for fluid mechanics. *Computers & Fluids*, *225*, 104973. https://doi.org/10.1016/j.compfluid.2021.104973

[6] Liu, F. Y., Gao, Y. T., Yu, X., Ding, C. C., Deng, G. F., & Jia, T. T. (2021). Painlevé analysis, Lie group analysis and soliton-cnoidal, resonant, hyperbolic function and rational solutions for the modified Korteweg-de Vries-Calogero-Bogoyavlenskii-Schiff equation in fluid mechanics/plasma physics. *Chaos, Solitons & Fractals*, *144*, 110559. https://doi.org/10.1016/j.chaos.2020.110559

[7] Brunton, S. L. (2021). Applying machine learning to study fluid mechanics. *Acta Mechanica Sinica*, *37*(12), 1718-1726. https://doi.org/10.1007/s10409-021-01143-6

[8] Alexandersen, J., & Andreasen, C. S. (2020). A review of topology optimisation for fluid-based problems. *Fluids*, *5*(1), 29. https://doi.org/10.3390/fluids5010029

[9] Elger, D. F., LeBret, B. A., Williams, B. C., Crowe, C. T., & Roberson, J. A. (2022). *Engineering Fluid Mechanics, International Adaptation*. John Wiley & Sons.

[10] Brunton, S. L., Noack, B. R., & Koumoutsakos, P. (2020). Machine learning for fluid mechanics. *Annual review of fluid mechanics*, *52*(1), 477-508. https://doi.org/10.1146/annurev-fluid-010719-060214